Global Biogeochemical Cycles

Supplementary Information for

The African Regional Greenhouse Gases Budget (2010-2019)

Yolandi Ernst[1], Sally Archibald[2], Frederic Chevallier[3], Philippe Ciais[3], Carlos Gonzalez Fischer[4], Benjamin Gaubert[5], Thomas Higginbottom[6], Steven Higgins[7], Shakirudeen Lawal[8], Fabrice Lacroix[9,10], Ronny Lauerwald[11], Mauro Lourenco[12,13], Carola Martens[14,15], Anteneh G. Mengistu[16], Lutz Merbold[17], Edward Mitchard[19], Mthokozisi Moyo[13], Hannah Nguyen[19], Michael O'Sullivan[20], Thais Rosan[21], Judith Rosentreter[22], Casey Ryan[7], Simon Scheiter[15], Stephen Sitch[21], Nicola Stevens[2,23], Torbern Tagesson[24,25], Hanqin Tian[26], Mengija Wang[27,28], Joel Woon[29], Bo Zheng[30,31], Yong Zhou[32,33], Robert J. Scholes[1]

[1] Global Change Institute, University of the Witwatersrand, Johannesburg, South Africa
[2] School of Animal, Plant and Environmental Sciences, University of the Witwatersrand, Johannesburg, Private Bag X3,WITS, 2050, South Africa
[3] Laboratoire des Sciences du Climat et de l'Environnement, LSCE/IPSL, CEA-CNRS-UVSQ, Université Paris-Saclay, Gif-sur-Yvette, France
[4] Department of Global Development, College of Agriculture and Life Sciences, Cornell University, Ithaca, NY, USA
[5] Atmospheric Chemistry Observations & Modeling Laboratory (ACOM), National Center for Atmospheric Research (NCAR), Boulder, CO
[6] School of GeoSciences, University of Edinburgh, Edinburgh, United Kingdom
[7] Plant Ecology, University of Bayreuth, Universitätsstraße 30, 95447 Bayreuth, Germany
[8] Department of Forestry and Environmental Resources, College of Natural Resources, North Carolina State University
[9] Climate and Environmental Physics, University of Bern, Bern, Switzerland
[10] Oeschger Centre for Climate Change Research (OCCR), University of Bern, Bern, Switzerland
[11] Université Paris-Saclay, INRAE, AgroParisTech, UMR ECOSYS, Palaiseau, France
[12] School of Geography, Archaeology and Environmental Studies, University of the Witwatersrand, South Africa.
[13] National Geographic Okavango Wilderness Project, Wild Bird Trust, South Africa
[14] Senckenberg Biodiversity and Climate Research Centre (SBiK-F), Senckenberganlage 25, 60325 Frankfurt am Main, Germany
[15] Institute of Physical Geography, Goethe University Frankfurt am Main, Altenhoeferallee 1, 60438 Frankfurt am Main, Germany
[16] Finnish Meteorological Institute, Helsinki, Finland
[17] Integrative Agroecology Group, Strategic Research Division Agroecology and Environment, Agroscope, Reckenholzstrsse 191, 8046 Zurich, Switzerland
[18] School of GeoSciences, King's Buildings, University of Edinburgh, Edinburgh EH9 3JN, UK
[19] Department of Geography, King's College London Strand, London WC2R 2LS, UK
[20] Faculty of Environment, Science and Economy, University of Exeter, Exeter EX4 4QF, UK
[21] College of Life and Environmental Sciences, University of Exeter, Exeter EX4 4RJ, UK
[22] Faculty of Science and Engineering, Southern Cross University, Lismore, NSW, Australia
[23] Environmental Change Institute, School of Geography and the Environment, University of Oxford, Oxford, UK

[24] Department of Physical Geography and Ecosystem Science, Lund University, Sölvegatan 12, SE-223 62 Lund, Sweden
[25] Department of Geosciences and Natural Resource Management, University of Copenhagen, Øster Voldgade 10, DK-1350 Copenhagen, Denmark
[26] School of Forestry and Wildlife Sciences, Auburn University, 602 Ducan Drive, Auburn, AL 36849, USA
[27] School of Geoscience and Technology, Zhengzhou University, 450001, China
[28] INRAE, UMR1391 ISPA, Universit´e de Bordeaux, F-33140 Villenave d'Ornon, France
[29] School of Environmental Sciences, University of Liverpool, Liverpool, UK
[30] Department of Earth System Science, Tsinghua University, Beijing 100084, China
[31] State Key Joint Laboratory of Environment Simulation and Pollution Control, School of Environment, Tsinghua University, Beijing 100084, China
[32] Department of Wildland Resources, Utah State University, Logan, Utah, 84321, USA
[33] Ecology Center, Utah State University, Logan, Utah, 84321, USA

Corresponding author(s):

Yolandi Ernst (yolandi.ernst@wits.ac.za)

Sally Archibald (sally.archibald@wits.ac.za)

Contents of this file

Figures

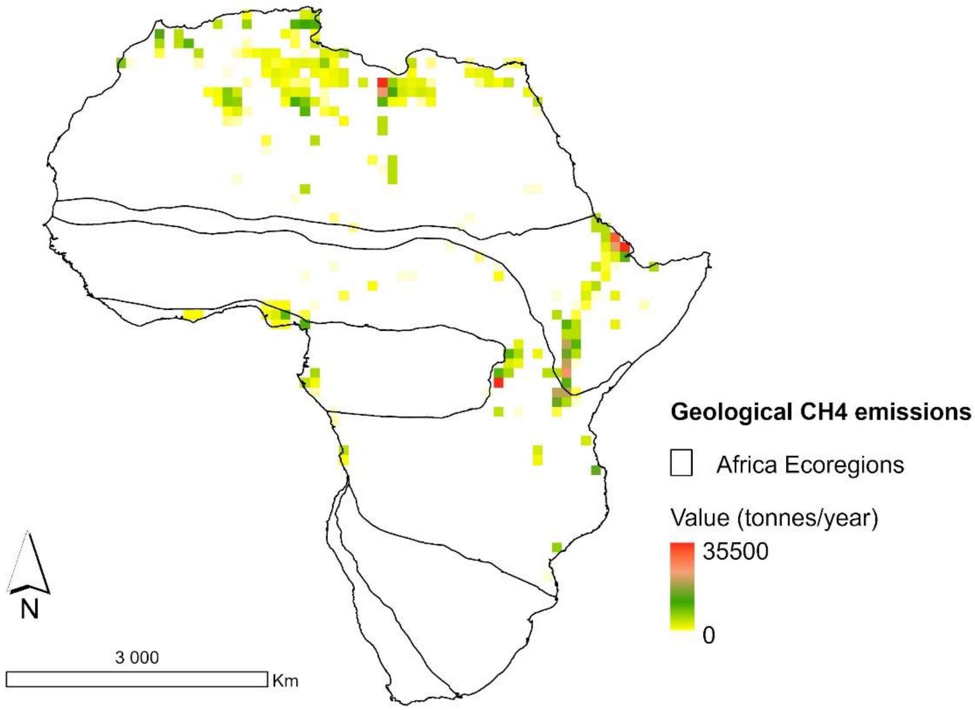

Figure S1. Estimates of geological CH4 emissions in Africa based on the gridded dataset of Etiope et al. (2019).

Tables

Table S1. Information and repositories on the data used for the estimation of aboveground biomass.

	McNicol	CCI Biomass	Brandt LVOD	NCEO
Reference	https://doi.org/10.1038/s41467-018-05386-z	https://doi.org/10.5194/essd-13-3927-2021	https://doi.org/10.1038/s41559-018-0530-6	In prep
Dataset	https://datashare.is.ed.ac.uk/handle/10283/3059	https://catalogue.ceda.ac.uk/uuid/5f331c418e9f4935b8eb1b836f8a91b8	https://matinbrandt.wordpress.com/data/	Soon to be made public
Technical information		https://climate.esa.int/en/projects/biomass/		https://leicester.figshare.com/articles/dataset/Africa_Aboveground_Biomass_map_for_2017/15060270
Notes	This analysis used a newer version of the model outputs which will be available shortly - paper in prep	More information on product available here		Data will be made public when the paper is published
Spatial resolution	25m	1km	25km	1km
Advantages	Uses real in-situ training data to model biomass and probabilistic approach to change detection (i.e. specifically designed to assess change)	Uses multiple data sources (C and L-band radar)	The L-VOD signal has sensitivity to high AGB	Lots of good height estimates, from the GEDI mission
Drawbacks	Very localised training site data, errors from soil moisture, does not validate change	Very little in-situ training data, and big regional biases. More training and model development required	Clear artefacts from soil moisture, pixels too large to assess product accuracy or train and validate	Very localised validation sites

Table S2. Vegetation gross primary productivity (GPP) products with their spatial and temporal resolution and estimates for Africa (± one standard deviation of inter-annual and model variability) for various time periods.

Models (spatial; temporal resolution)	Period	Mean GPP (PgC)	Trend GPP ($TgCy^{-1}$)	Mean	IAV*	Trend *
LRF-GPP (0.05°×0.05°, Daily)[1]	1982-2015	26.1 ± 0.8	55.5 ± 110.8	21.4 ± 0.7	27.4 ± 3.8	20.7 ± 4.1
	2000-2015	26.5 ± 0.5	-15.0 ± 26.5	21.4 ± 0.4	33.8 ± 7.6	6.6 ± 11.7
	1985-2009	26.2 ± 0.7	62.8 ± 135.1	21.5 ± 0.5	23.6 ± 3.8	26.3 ± 5.7
	2009-2015	26.4 ± 0.5	-102.1 ± 877.9	21.2 ± 0.4	16.3 ± 18.2	27.0 ± 23.2
FLUXCOM (0.5°×0.5°, Monthly)[2]	1982-2015	24.8 ± 0.3	20.0 ± 47.0	21.6 ± 0.3	27.9 ± 11	41.3 ± 9.7
	2000-2015	21.8 ± 0.2	24.3 ± 10.9	21.8 ± 0.2	15.8 ± 9.8	30.6 ± 13.7
	1985-2009	24.8 ± 0.3	17.2 ± 62.9	21.7 ± 0.2	27.6 ± 11.1	38.5 ± 14.1
	2009-2015	25.0 ± 0.1	-7.8 ± 513.9	21.8 ± 0.1	15.6 ± 15.1	4.2 ± 27.6
K Smith (0.5°×0.5°, Monthly)[3]	1982-2015	20.7 ± 0.3	9.3 ± 50.6	20.1 ± 0.3	25.2 ± 4.5	11.1 ± 6.1
	2000-2015	20.7 ± 0.2	22.2 ± 11.8	20.0 ± 0.2	13.7 ± 8.7	21.1 ± 11.2
	1985-2009	20.7 ± 0.2	-3.6 ± 68.3	20.2 ± 0.2	20.9 ± 5.4	4.7 ± 8.9
	2009-2015	20.8 ± 0.2	-5.4 ± 359.5	20.0 ± 0.2	18.8 ± 9.2	1.5 ± 10.0
P-model (0.5°×0.5°, Daily)[4]	1982-2015	22.1 ± 1.0	91.8 ± 80.1	17.7 ± 0.8	19.3 ± 5.8	20.2 ± 1.8
	2000-2015	22.9 ± 0.4	54.1 ± 20.5	17.8 ± 0.3	13.6 ± 9.3	14.8 ± 5.6
	1985-2009	22.1 ± 0.8	92.3 ± 91.2	17.8 ± 0.6	12.6 ± 6.4	22.2 ± 2.2
	2009-2015	23.1 ± 0.4	-4.3 ± 770.1	17.7 ± 0.3	18.6 ± 9.8	0.9 ± 16
MOD17 (0.5°×0.5°, Monthly)[5]	2000-2015	23.1 ± 0.5	50.0 ± 24.7	20.3 ± 0.4	39.4 ± 14.5	19.6 ± 9.7
	2009-2015	23.4 ± 0.4	-3.4 ± 763.5	20.4 ± 0.3	22.1 ± 22.5	0.6 ± 14.0
SMAP (9×9 km2, daily)[6]	2000-2015	25.3 ± 0.8	133.5 ± 28.4	20.3 ± 0.7	27.1 ± 9.2	24.5 ± 5.2
	2009-2015	26.0 ± 0.4	-20.5 ± 858.9	20.7 ± 0.3	22.5 ± 11.7	3.0 ± 12.7
VPM (0.05°×0.05°, 8-day)[7]	2000-2015	27.7 ± 0.6	95.2 ± 25.3	22.1 ± 0.5	9.8 ± 17.7	16.7 ± 4.4
	2009-2015	28.2 ± 0.5	16.4 ± 1028.0	22.2 ± 0.4	1.8 ± 42.6	1.8 ± 11.2
All models	1982-2015	23.4 ± 0.6 ± 2.5	39.7 ± 68.1 ± 37.4	20.2 ± 0.5 ± 1.8	7.2 ± 1.3 ± 4.0	18.2 ± 3.1 ± 12.7
	2000-2015	24.0 ± 0.4 ± 2.4	48.4 ± 18.8 ± 49.4	20.5 ± 1.5 ± 1.5	36.1 ± 2.1 ± 11.5	15.0 ± 5.4 ± 7.6
	1985-2009	23.4 ± 0.4 ± 2.5	42.2 ± 72.5 ± 43.5	20.2 ± 0.3 ± 1.8	7.5 ± 1.1 ± 6.4	24.3 ± 4.2 ± 14.0
	2009-2015	24.7 ± 0.3 ± 2.5	-31.6 ± 609.2 ± 38.6	20.5 ± 0.3 ± 1.5	37.1 ± 3.5 ± 7.0	4.9 ± 9.4 ± 9.5

[1] (Tagesson et al. 2021); [2] (Jung et al., 2011); [3] (Kolby Smith et al., 2015); [4] (Stocker et al., 2019); [5] (Running et al., 2004); 6 (Jones et al., 2017); 7 (Zhang et al., 2017)

Note. Trends and IAV in the RECCAP2 period should be used cautiously because of the short study period, but is still included for consistency.

Table S3. Carbon stocks and fluxes simulated by aDGVM. Variables are averaged for whole Africa and ecoregions for the periods 1985-2008 (R1) and 2009-2018 (R2). Trends were derived by linear regression models for the two periods using time series of monthly means of the respective variable. Some values in the table are zero due to rounding.

		Total (PgC)		**Per area (kgCm^{-2})**		**Trend (PgCyr^{-1})**	
Carbon stocks	**Region**	**R1**	**R2**	**R1**	**R2**	**R1**	**R2**
Aboveground live carbon	NA Desert	0.72	0.78	0.07	0.08	0.003	0.01
	Forest	17.25	17.93	7.31	7.6	0.038	0.043
	Desert/shrubland	0.2	0.22	0.29	0.32	0.001	0.001
	Sub-humid savanna	23.74	26.09	2.38	2.62	0.124	0.169
	Semi-arid savanna	5.13	5.83	0.84	0.96	0.033	0.042
	Whole Africa	47.03	50.84	2.18	2.31	0.199	0.264
Aboveground dead carbon	NA Desert	0.23	0.27	0.02	0.03	0.003	0.006
	Forest	1.6	1.73	0.68	0.73	0.006	0.009
	Desert/shrubland	0.06	0.07	0.09	0.1	0	0
	Sub-humid savanna	4.46	4.88	0.45	0.49	0.022	0.033
	Semi-arid savanna	1.56	1.75	0.26	0.29	0.008	0.01
	Whole Africa	7.92	8.7	0.3	0.33	0.039	0.057
Belowground live carbon	NA Desert	0.59	0.67	0.06	0.07	0.005	0.012
	Forest	3.67	3.91	1.56	1.66	0.013	0.01
	Desert/shrubland	0.13	0.15	0.2	0.22	0.001	0
	Sub-humid savanna	11.65	12.88	1.17	1.29	0.061	0.086
	Semi-arid savanna	3.9	4.4	0.64	0.72	0.023	0.025
	Whole Africa	19.95	22.02	0.73	0.79	0.101	0.133
Belowground dead carbon	NA Desert	0	0	0	0	0	0
	Forest	0.01	0.01	0	0	0	0
	Desert/shrubland	0	0	0	0	0	0
	Sub-humid savanna	0.03	0.03	0	0	0	0
	Semi-arid savanna	0.01	0.02	0	0	0	0
	Whole Africa	0.06	0.06	0	0	0	0
Soil carbon	NA Desert	4.22	4.33	0.42	0.43	0.006	0.012
	Forest	12.75	13.29	5.4	5.63	0.027	0.039
	Desert/shrubland	1	1.03	1.47	1.52	0.001	0.003
	Sub-humid savanna	39.32	40.98	3.95	4.12	0.081	0.117
	Semi-arid savanna	16.37	17.15	2.7	2.82	0.032	0.049
	Whole Africa	73.66	76.77	2.79	2.9	0.147	0.219
		Total (PgCyr^{-1})		**Per area (gC/m^2/day)**		**Trend (PgCyr^{-1})**	
Carbon fluxes	**Region**	**R1**	**R2**	**R1**	**R2**	**R1**	**R2**
Autotrophic respiration	NA Desert	0.02	0.02	0	0	0	0
	Forest	0.33	0.37	0.38	0.42	0.002	0.002
	Desert/shrubland	0	0	0.02	0.02	0	0
	Sub-humid savanna	0.56	0.65	0.15	0.18	0.005	0.01
	Semi-arid savanna	0.13	0.16	0.06	0.07	0.001	0.003
	Whole Africa	1.03	1.19	0.12	0.14	0.008	0.015
Heterothrophic respiration	NA Desert	0.34	0.39	0.09	0.1	0.003	0.005
	Forest	1.39	1.49	1.62	1.73	0.005	0.008
	Desert/shrubland	0.11	0.12	0.44	0.49	0	0.001
	Sub-humid savanna	4.37	4.72	1.2	1.3	0.018	0.026
	Semi-arid savanna	1.9	2.1	0.86	0.95	0.008	0.01
	Whole Africa	8.11	8.82	0.84	0.91	0.033	0.051

Table S4. Fuelwood emissions estimates from literature sources and the IEA world energy balances 2020. The World Energy Balances statistics reported in Ktoe were converted to fuel use (in Tg) using a conversion rate of 2460g dry wood/Ktoe (Scholes 2011), biomass was converted to carbon using a conversion of 0.45gC per g wood biomass. Biomass was converted to carbon using a conversion of 0.45gC per g wood biomass.

Source	Reference	Year	Ktoe	Fuel use (Tg)	C emissions	CO2 emissions
FAO	Amos, 1999 in Scholes 2011	1990		317	143	523
IEA	IEA World Energy Balances 2020	1990	133169	328	147	541
BEST	Amous, 1999 in Scholes 2011	1994		451	203	744
IEA	IEA World Energy Balances 2020	1995	153488	378	170	623
WEIS	Amous, 1999 in Scholes 2011	1996		418	188	690
FAO	Amous, 1999 in Scholes 2011	1999		371	167	613
FAO	Broadhead 2001 in Scholes 2011	2000		452	203	746
Bailis	Bailis 2005 in Scholes 2011	2000		470	212	776
IEA	IEA World Energy Balances 2020	2000	168820	415	187	685
FAO	FAO 2010 in Scholes 2011	2005		430	193	709
IEA	IEA World Energy Balances 2020	2005	193603	476	214	786
FAO	FAO 2010 in Scholes 2011	2010		493	222	813
FAO Charcoal transition	Boden 2013 in FAO Charcoal transition	2010			223	817
IEA	IEA World Energy Balances 2020	2010	217653	535	241	883
Bailis	Bailis et al 2015	2012		438	197	723
IEA	IEA World Energy Balances 2020	2015	248245	611	275	1008
IEA	IEA World Energy Balances 2020	2018	265047	652	293	1076

Table S5: Estimated emissions factors and mass for free-ranging cattle reported by various sources. The latest IPCC 2019 value is an outlier here and results in almost double previously reported estimates of livestock methane emissions for Africa.

	Average methane emissions factor ($kgCH_4$ $head^{-1}$ yr^{-1})	Herd-composition adjusted mass per head (kg)
IPCC1997	32.0	250
IPCC2006	31.0	250
Herrero 2008	31.1	250
Goopy 2018	27.5	186
IPCC2019	48.0	248
Ndungu 2020	39.8	248
Ndungu 2021	40.0	228
mean	**35.6**	**237.1**
stdev	**7.2**	**23.9**

Table S6. Summary of field measurements of CH_4 emission rates from termites at individual species and mound scales across African continent.

Reference	Location	Ecosystem	Scale	Species	Methane emission rate
Nyamadzawo et al., (2012)	Zimbabwe	Wetland	Mound	*Odontoterme transvaalensis*	778 μg CH_4 m^{-2} h^{-1}
Brümmer et al., (2009)	Burkina Faso	Savanna	Mound	*Cubitermes fungifaber*	2849 μg CH_4 m^{-2} h^{-1}
Brauman et al., (2001)	Cameroon	Savanna	Individual	*Schedorhinotermes putorius*	1.52 μg CH_4 g^{-1} h^{-1}
				Termes hospes	12.83 μg CH_4 g^{-1} h^{-1}
				Astalotermes quietus	3.36 μg CH_4 g^{-1} h^{-1}
				Pericapritermes chiasognatus	5.14 μg CH_4 g^{-1} h^{-1}
				Ophiotermes grandilabius	2.39 μg CH_4 g^{-1} h^{-1}
				Thoracotermes macrothorax	3.85 μg CH_4 g^{-1} h^{-1}
				Coxotermes bukokoensis	4.85 μg CH_4 g^{-1} h^{-1}
				Termes hospes	12.83 μg CH_4 g^{-1} h^{-1}
	Republic of Congo	Savanna	Individual	*Nasutitermes lujae*	2.62 μg CH_4 g^{-1} h^{-1}
				Microcerotermes parvus	0.68 μg CH_4 g^{-1} h^{-1}
	Chad	Savanna	Individual	*Macrotermes subhyalinus*	1.84 μg CH_4 g^{-1} h^{-1}
MacDonald et al., 1998	Cameroon	Primary forest	Mound	*Astalotermes quietus*	143 ng CH_4 s^{-1} $mound^{-1}$
				Procubitermes arboricola	968 ng CH_4 s^{-1} $mound^{-1}$
				Cephalotermes rectangularis	467 ng CH_4 s^{-1} $mound^{-1}$
				Cubitermes bulbifrons	1808 ng CH_4 s^{-1} $mound^{-1}$
				Astalotermes spp.	125 ng CH_4 s^{-1} $mound^{-1}$
		Secondary forest	Mound	*Astalotermes quietus*	212 ng CH_4 s^{-1} $mound^{-1}$
				Cubitermes bulbifrons	5478 ng CH_4 s^{-1} $mound^{-1}$
				Cubitermes gaigei	1660 ng CH_4 s^{-1} $mound^{-1}$
				Procubitermes arboricola	168 ng CH_4 s^{-1} $mound^{-1}$
				Astalotermes spp.	81 ng CH_4 s^{-1} $mound^{-1}$
				Cephalotermes rectangularis	312 ng CH_4 s^{-1} $mound^{-1}$
MacDonald et al., 1998	Cameroon	Forest	Mound	*Thoracotermes macrothorax*	636 ng CH_4 s^{-1} $mound^{-1}$
				Cubitermes fungifaber	53.4 ng CH_4 s^{-1} $mound^{-1}$
Rouland et al. 1993	Republic of Congo		Individual	*Microcerotermes parvus*	2.24 μg CH_4 g^{-1} h^{-1}
				Nasutitermes lujae	2.40 μg CH_4 g^{-1} h^{-1}
				Nasutitermes arborum	2.08 μg CH_4 g^{-1} h^{-1}
				Trinervitermes rhodensiensis	0.34 μg CH_4 g^{-1} h^{-1}
				Pseudacanthotermes militaris	14.08 μg CH_4 g^{-1} h^{-1}
				Pseudacanthotermes spiniger	6.72 μg CH_4 g^{-1} h^{-1}
				Macrotermes muelleri	5.60 μg CH_4 g^{-1} h^{-1}
				Macrotermes bellicosus	6.72 μg CH_4 g^{-1} h^{-1}
				Noditermes sp.	10.24 μg CH_4 g^{-1} h^{-1}
				Crenetermes albotarsalis	14.88 μg CH_4 g^{-1} h^{-1}
				Cubitermes speciosus	14.24 μg CH_4 g^{-1} h^{-1}
				Thoracotermes macrothorax	17.44 μg CH_4 g^{-1} h^{-1}
				Astratotermes sp.	8.48 μg CH_4 g^{-1} h^{-1}

Table S7. Methane emission estimates ($TgCH_4yr^{-1}$) for different geological sources across Africa and the Scholes African Ecoregions.

Ecoregion	**Onshore seeps (OS)**	**Microseepage (MS)**	**Geothermal Manifestations (GM)**	**Total**
NA Desert	0.00121	0.370179	0.0965	0.467889
Forest	0.00402	0.031205	0.011	0.046225
Desert/shrubland	0	0	0	0
Sub-humid savanna	0.0171	0.054506	0.129	0.200606
Semi-arid savannna	0.006	0.011034	0.2825	0.299534
Africa	0.02833	0.466924	0.519	1.014254

Note. Estimates calculated from gridded maps produced by Etiope et al., 2019.

Table S8. Estimates of the CO_2 uptake from geological weathering and DIC release through run-off as calculated from gridded products provided by Lacroix et al. (2020)

	CO_2 uptake ($TgCyr^{-1}$)	**DIC release ($TgCyr^{-1}$)**
NA desert	0.153	0.209
Forest	1.605	2.070
Desert/shrubland	0.282	0.362
Sub-humid savanna	7.710	9.618
Semi-arid savanna	2.182	2.648
Africa	**12.236**	**15.210**